Pergamon

Journal of Structural Geology, Vol. 16, No. 2, pp. 203 to 221, 1994
Copyright © 1994 Elsevier Science Ltd
Printed in Great Britain. All rights reserved
0191-8141/94 $06.00 + 0.00

Preservation and evolution of quartz phenocrysts in deformed rhyolites from the Proterozoic of southwestern North America

M. L. Williams and J. L. Burr

Department of Geology and Geography, University of Massachusetts, Amherst, MA 01003, U.S.A.

(*Received 6 January 1993; accepted in revised form 6 April 1993*)

Abstract—Euhedral quartz phenocrysts (quartz eyes) are well preserved in ductilely deformed Proterozoic metarhyolites in southwestern North America. In a single sample, the phenocrysts can range from undeformed to highly deformed and recrystallized. Matrix fabrics are extremely similar to those in undeformed ash-flow tuffs. The preservation of the phenocrysts reflects an efficient partitioning of strain from the phenocrysts into the fine-grained, wet and possibly glassy matrix. Variations in the degree of phenocryst deformation involve: (1) the chemical and mechanical character of the original phenocryst; (2) the degree to which matrix water has access to the quartz crystal; and (3) crystallographic orientation.

Phenocryst-bearing metarhyolites are relatively strain-insensitive, but they contain important kinematic information even in recrystallized rocks where constraints on early structural events are rare. Most phenocrysts have asymmetrical tails, shadows, or deflected matrix foliations that indicate a consistent sense of shear throughout a sample or outcrop. These deformation-induced fabrics are readily distinguishable from primary fabrics in all but the lowest grade samples. In the Tusas Mountains of northern New Mexico and in the Shylock fault zone of central Arizona, quartz-eye metarhyolites have been useful in differentiating early thrusting and shortening events from later syn-metamorphic events that dominate the microstructures and obscure the early tectonic history.

INTRODUCTION

Fine-grained felsic schists and gneisses with dispersed, euhedral quartz crystals ('quartz eyes') have been described from a variety of geologic terranes. They are particularly common in association with volcanogenic massive sulfide deposits (Hopwood 1976, Vernon 1986a), and a large body of literature has been devoted to their significance for ore genesis (e.g. Goodspeed 1937, Hopwood 1977, Frater 1983). Controversy has surrounded the interpretation of these rocks (Gresens & Stensrud 1974, DeRosen-Spence & Spence 1977, Hopwood 1977, Vernon & Flood 1977, Vernon 1986a). At least three alternative interpretations have been suggested for the quartz eyes. They may represent: (1) metamorphic porphyroblasts; (2) relict phenocrysts in deformed volcanic rocks; or (3) porphyroclasts in tectonites or mylonites. Although alternative models may apply to some occurrences, Vernon (1986a,b) concluded that virtually all microstructures are consistent with an origin as primary phenocrysts in volcanic rocks. Thus, unlike deformed granitoids where quartz is one of the most readily deformable minerals, quartz phenocrysts in volcanic rocks can apparently survive intense ductile deformation and, in many rocks, maintain primary volcanic characteristics (Etheridge & Vernon 1981, Vernon 1986a, Williams & Burr 1990).

'Quartz-eye' schists and gneisses are an important component of the Proterozoic supracrustal section of southwestern North America. They occur in a variety of deformational and metamorphic settings ranging from the brittle (sub-greenschist facies) to the ductile (amphibolite facies) regimes. Euhedral quartz crystals can occur across a broad range of fabrics and, in many rocks, highly deformed and essentially undeformed quartz crystals coexist. Although few workers have questioned the volcanic origin of the quartz and feldspar megacrysts, many aspects of the origin and evolution of the associated microstructures are less clear. Two that are particularly important for structural analysis are: (1) the degree to which the microstructures reflect volcanic rather than deformational processes; and (2) the processes that allow the nearly euhedral quartz phenocrysts to persist through ductile deformation and metamorphism.

The purpose of this paper is to summarize the microstructural characteristics of deformed felsic metavolcanic rocks from a variety of settings and to place constraints on the origin and evolution of the fabrics, especially those related to the quartz and feldspar phenocrysts. The results suggest that the deformational fabrics are generally distinguishable from primary fabrics in all but the lowest grade samples, and that several factors may contribute to the relative strength of the phenocrysts. An important consequence of the study is the suggestion that phenocryst-bearing volcanic rocks, although unreliable as indicators of strain magnitude, are useful kinematic indicators, especially in multiply deformed supracrustal sequences where early fabrics are obscured by later metamorphism and recrystallization.

GEOLOGIC SETTING

Volcanic rocks investigated in this study were collected from Proterozoic exposures in north-central New Mexico and the Transition Zone of Arizona (Fig. 1). These rocks are part of a broad Early to Late Protero-

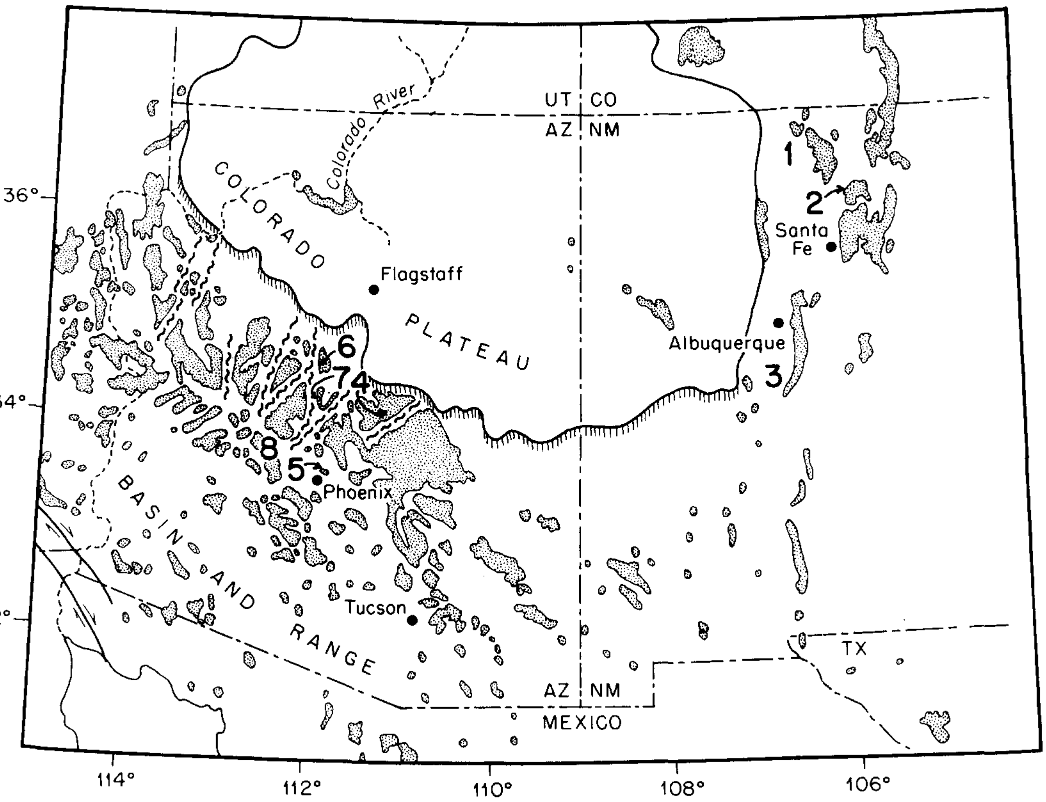

Fig. 1. Location map for Proterozoic rocks in southwestern North America showing the general locations of deformed felsic volcanic rocks sampled or investigated in this study. Formation names, metamorphic conditions and relevant references are presented for each area in Table 1.

zoic orogenic zone that extends from SE California to Labrador (Hoffman 1988). Supracrustal rocks range in age from approximately 1.75 to 1.6 Ga (Karlstrom & Bowring 1991, Robertson *et al.* in press). They can be divided into three generally age-correlative lithotectonic groups: (1) 1.75–1.72 Ga arc-related sequences dominated by mafic metavolcanic and immature metasedimentary rocks, including the Yavapai Supergroup in central Arizona (Anderson & Blacet 1972, P. Anderson 1989, Karlstrom & Bowring 1991) and the Moppin, Pecos and Gold Hill Complexes in northern New Mexico (Bauer & Williams 1989, Robertson & Condie 1989, Robertson *et al.* in press); (2) 1.72–1.69 Ga sequences dominated by massive orthoquartzite and metamorphosed rhyolite, including the Mazatzal Group in Arizona (Conway & Silver 1989) and the Hondo Group in New Mexico (Bauer & Williams 1989); and (3) 1.69–1.60 Ga volcanic and sedimentary rocks exposed primarily in southeastern Arizona (Karlstrom & Bowring 1991) and in central New Mexico (Robertson *et al.* in press). Although the samples chosen for this study come from all three groups, the second (1.72–1.69 Ga) is particularly well known for its thick sequences of metamorphosed felsic volcanic rocks (Conway 1976, Robertson *et al.* in press).

Karlstrom & Bowring (1991) identified three major pulses of convergent tectonism in Arizona at 1.74 Ga, 1.70 Ga (Yavapai orogeny) and 1.66–1.60 Ga (Mazatzal orogeny). Uncertainties remain about the timing of deformation and metamorphism in New Mexico (Williams 1990, Robertson *et al.* in press), but it is likely that one or more pulses of convergent deformation occurred between 1.7 and 1.6 Ga with other fabric-forming events occurring as late as 1.4 or 1.3 Ga (Robertson *et al.* in press). Most supracrustal rocks have strong ductile deformation fabrics, typically with an early, nearly bedding-parallel foliation that is interpreted to reflect thrust-related shearing, and a heterogeneous array of discordant fabrics associated with later folding events (Bauer 1988, Williams 1990, Karlstrom & Bowring 1991). In felsic volcanic rocks, early layer-parallel fabrics are particularly well-developed, but later discordant fabrics are more heterogeneously developed. Apparently, the later events were partitioned into more schistose rocks.

Most of the Proterozoic rocks were metamorphosed to greenschist or amphibolite facies. Peak conditions were similar over large areas (Grambling *et al.* 1989, Williams 1990). Across Arizona, peak pressures were near 3 kbar. Peak temperatures varied from less than 400°C to more than 700°C, but high temperature regions are interpreted to reflect the effects of syn-tectonic plutonism (Williams 1991b). Most regions in northern and central New Mexico preserve peak metamorphic conditions near the Al_2SiO_5 triple point (500°C, 4 kbar), but greenschist facies terranes are present in the northern Tusas Mountains and in central New Mexico. Peak conditions are interpreted to be syn-tectonic, but they seem to have occurred late in the deformation history of most regions. The layer-parallel fabrics were formed

Table 1. Sample localities for quartz phenocryst-bearing volcanic rocks

Locality	N*	Formation	Age	T/P (°C, kbar)†	References
Tusas Mountains, New Mexico —northern	1	Burned Mountain Formation	1.7 Ga	450, 3.0	Bauer & Williams (1989) Williams (1987) Barker (1958)
Tusas Mountains, New Mexico —southern	1	Vadito Group	1.7 Ga	500–600, 4.0	Williams (1987) Bingler (1965)
Picuris Mountains, New Mexico —western	2	Glen Woody Formation	1.7 Ga	500, 3.8	Bauer & Williams (1989) Bauer (1988)
Manzano Mountains, New Mexico	3	Unnamed	~1.65 Ga	400–500, 4.0	Bauer (1983) Thompson *et al.* (1991)
Mazatzal Mountains, Arizona	4	Red Rock/Rhyolite	~1.7 Ga	200–400, 2.0	Conway (1976) Conway & Silver (1989) Gillentine *et al.* (1991)
Squaw Peak, Phoenix Mountains, Arizona	5	Unnamed	~1.7 Ga	420, 2.5	Thorpe (1980) Thorpe & Burt (1978) Karlstrom *et al.* (1990)
Jerome–Prescott, Arizona	6	Cleopatra rhyolite	~1.74 Ga	400, 3.0	
East Bradshaw Mountains, Arizona —Crazy Basin area to —Black Canyon City	7	Unnamed rhyolite—near Shylock fault zone	~1.74–1.72 Ga	450, 3.0	Darrach (1989) Darrach *et al.* (1991) Jerome (1956)
Hieroglyphic Mountains, Arizona	8	Unnamed	~1.74–1.72 Ga	450, 3.0	Burr (1991, 1992)

*Numbers keyed to Fig. 1.
†Estimated temperature and pressure at metamorphic peak.

earlier in the prograde metamorphic history (Williams 1991a).

We investigated Proterozoic volcanic rocks from a variety of regions and geologic settings in New Mexico and Arizona (Fig. 1 and Table 1). However, detailed field and laboratory studies were carried out in several principal areas. These include: the Vadito Group in northern New Mexico; the Yavapai Supergroup in the Southern Hieroglyphic Mountains and eastern Bradshaw Mountains, central Arizona; the Red Rock Rhyolite, Mazatzal Mountains, Arizona; and quartz phenocryst-bearing rhyolite from Squaw Peak in Phoenix, Arizona. Geologic investigations have been carried out by other workers in each of these areas (see references in Table 1), and the quartz-eye rocks in each area have been interpreted as metamorphosed volcanic rocks or volcanogenic sediments.

CHARACTERISTICS OF DEFORMED 'QUARTZ-EYE' VOLCANIC ROCKS

Deformed felsic volcanic rocks have a remarkably similar macroscopic and microscopic character. They have a fine-grained, well-foliated, quartzo-feldspathic matrix and dispersed quartz and feldspar 'eyes', 1–2 orders of magnitude larger than the matrix grains (Fig. 2a). The matrix is dominated by quartz and muscovite (commonly phengitic) with smaller amounts of chlorite, plagioclase, and hematite–ilmenite. Trace amounts of epidote, piemontite, zircon, sphene, magnetite, rutile, tourmaline and apatite have been noted. Although plagioclase and K-feldspar phenocrysts are ubiquitous, matrix K-feldspar is rare or absent, presumably having been removed by hydrothermal alteration or metamorphic reactions.

Most samples have a moderate to strong foliation and a strong mineral lineation (Fig. 2b). The matrix can be extremely fine-grained; quartz grains are typically 1–5 μm, even in amphibolite-grade rocks. Muscovite and hematite crystals, generally less than 20 μm in length, are well-foliated. Matrix quartz grains are typically inequant, with length to width ratios near 2:1, and are aligned with the foliation. They tend to be recrystallized, and grain boundaries, when the grains are coarse enough to be viewed optically, are straight with 120° triple junctions. Typically, quartz–quartz grain boundaries are pinned at the ends of muscovite or hematite crystals.

The matrix of most samples is crudely layered (Fig. 2b). Layers are defined by varying quartz:muscovite ratios, the percentage of muscovite ranging from zero to more than 50%. The layers anastomose across the rocks, wrapping around phenocrysts and quartz-rich pods. Both quartz-rich and muscovite-rich layers are discontinuous. Some of the layering undoubtedly represents primary compositional and textural heterogeneity, but some also reflects heterogeneous dissolution of matrix quartz due to the partitioning of strain into high- and low-strain domains. This effect is well illustrated near phenocrysts where high-strain domains can consist of nearly pure muscovite (Fig. 2c).

The presence of dispersed quartz eyes is the most characteristic feature of the quartzofeldspathic tectonites. Most are 1–3 mm in diameter and a typical thin section may contain as few as five or as many as 50 or more crystals. In most samples, some crystals have elliptical cross-sections and exhibit undulose extinction, deformation lamellae and subgrains while others are subhedral to euhedral with little or no evidence for internal strain (Fig. 2d). Many of the quartz crystals contain either circular or lobate re-entrants of fine-grained matrix material that are similar to, and almost certainly originated as, primary volcanic embayments (Figs. 2b & c). Significantly, the embayment-filling material is mineralogically similar to the matrix, but displays little or no foliation. This is an important piece of evidence used by Etheridge & Vernon (1981) and Vernon (1986a) to suggest that the eyes were phenocrysts not porphyroblasts which overgrew and included the matrix material.

Feldspar phenocrysts are also common, but most are distinctly altered and deformed (Figs. 2c & d). They typically contain visible muscovite or 'sericite', but even the cleanest feldspar grains have a cloudy or mottled appearance, interpreted to be the result of submicroscopic alteration. The feldspar phenocrysts tend to be angular in shape, and many show evidence of fracture and slip on crystallographic cleavage planes.

Most quartz and feldspar phenocrysts are associated with dramatic tails or shadows in the adjacent matrix material (Figs. 2b & c). The shadows generally have more quartz and weaker fabrics than the average matrix. Close to the phenocrysts, the foliation in the shadows occurs at an angle to that in the matrix. Away from the phenocryst, the foliation increases in intensity and curves progressively into the matrix orientation. The shadows are interpreted to be low-strain domains ('strain shadows') that have been protected from some of the bulk strain by the adjacent phenocryst. They can be symmetrical with respect to the phenocryst, but most are distinctly asymmetrical with a sigma geometry (Passchier & Simpson 1986). Delta geometries, interpreted to result from porphyroclast rotation (Passchier & Simpson 1986), have not been recognized. It is important to note that the strain shadows are unlike the tails associated with porphyroclasts in typical quartzo-feldspathic mylonites. Many contain little or no dynamically recrystallized porphyroclast material (i.e. recrystallized quartz from the quartz phenocryst), but instead, are entirely defined by matrix material.

Strongly foliated, mica-rich domains, 'quarter mats' (Hanmer & Passchier 1991), also occur near some phenocrysts (Fig. 2c). In lineation-parallel sections, the mats occur adjacent to phenocrysts in opposite quadrants, 'quarters' (Hanmer & Passchier 1991), from the strain shadows. These are interpreted to be high-strain domains from which quartz has been progressively removed during the deformation. The presence of these high-strain domains supports the strain shadow interpretation for the tails described above, and emphasizes the strength of the quartz phenocrysts relative to the matrix material.

One final observation may be particularly important for kinematic analysis and strain analysis. Several deformed volcanic rocks have been sampled from high-strain zones formed during late-stage deformational events. In these samples, the dominant foliation represents S_2 or S_3, and is a later fabric than that in other samples from the same area. However, microstructural characteristics of these samples are typically indistinguishable from those in samples dominated by S_1. Transposition can apparently occur very efficiently in phenocryst-bearing felsic volcanic rocks with little noticeable effect on the matrix or the phenocrysts.

COMPARISON WITH UNDEFORMED VOLCANIC ROCKS

A wide variety of fabrics have been described from 'undeformed' felsic volcanic rocks (Schmincke & Swanson 1967, Elston & Smith 1970, Rhodes & Smith 1972, Chapin & Lowell 1979, Wolff & Wright 1981), and many are analogous to those produced during solid-state ductile deformation (compare Figs. 2 and 3). However, important differences allow the ductile deformational fabrics to be distinguished from primary fabrics in most samples. As with plutonic rocks (Patterson *et al.* 1989), it is critical to distinguish primary from deformational structures before interpretations are made about the conditions of deformation or the kinematic history. Tertiary ash-flow tuffs from the Mogollon Datil Volcanic Field (Elston 1984, Ratte' *et al.* 1984) in southwestern New Mexico bear a striking resemblance to the deformed volcanic rocks; the high-silica Bloodgood Canyon Tuff (Rhodes 1976, Elston 1984) is particularly useful for comparison (Fig. 3). Table 2 summarizes several of the most distinctive microstructural features of the deformed and undeformed volcanic rocks.

Microstructures associated with phenocrysts

Quartz phenocrysts in undeformed ash-flow tuffs are strikingly similar to those in the deformed rocks. In both settings, they range from euhedral to anhedral, and the anhedral phenocrysts can be either angular or elliptical in cross-section (Figs. 4a & b). Volcanic embayments are virtually indistinguishable, even when comparing the most highly deformed Proterozoic rocks to undeformed Tertiary rocks. However, in Tertiary volcanic rocks, the quartz phenocrysts display little or no evidence for lattice strain regardless of morphology; slight undulose extinction has been observed in several phenocrysts. A broad range of deformational substructure is present in the deformed rocks, and the degree of development of substructure crudely correlates with the external morphology of the phenocryst. The most anhedral crystals tend to be the most deformed. This suggests that the processes leading to the development of anhedral phenocrysts in the Proterozoic rocks *can* include dynamic recrystallization resulting from dislocation glide and creep. In contrast, production of anhedral phenocrysts in undeformed rocks is related to fracturing due to interaction with other grains and to

Table 2. Comparison of microstructures in primary volcanic and deformed felsic volcanic rocks

Microstructure	Primary volcanic rocks	Deformed volcanic rocks
Quartz phenocrysts		
—Morphology	Anhedral to euhedral —some anhedral crystals elliptical but most are angular fragments	Anhedral to euhedral —anhedral crystals typically elliptical or lentil-shaped
—Embayments	Embayments common —contain structureless matrix material	Embayments common —contain isotropic matrix material
—Internal substructure	Minimal substructure —some undulatory extinction	Range from undeformed to strongly recrystallized —general correlation between shape and intensity of substructure
—Interfaces	Straight sharp interfaces with matrix material	Interfaces straight at low magnification, but irregular and recrystallized at high magnification —locally overgrow matrix phases
Feldspar phenocrysts		
—Morphology	Blocky crystals —commonly fractured along cleavage planes and dispersed	Blocky to irregular crystals —commonly fractured along cleavage planes and dispersed
—Alteration/metamorphism	Unaltered to moderately altered —alteration assemblage includes fine Fe-oxides and clay minerals	Most crystals are partly to mostly replaced by fine muscovite
Matrix microstructures		
—Foliation	Weak to strong foliation —defined by aligned crystals, fragments, pumice, etc., and by compositional banding	Variably developed —defined by aligned muscovite, hematite, and elongate quartz crystals, quartz ribbons, strain shadows, and compositional banding
—Interaction with phenocrysts	Asymmetric tails and shadows defined by disturbance of matrix flow, around phenocrysts —complex internal fabrics within the tail —tails heterogeneously developed even on a single phenocryst	Well-developed strain shadows present on most phenocrysts —consist of quartz-rich, low strain domains with regularly curving internal foliation —mica-rich high-strain domains occur on opposite quadrants

resorption due to heating or undercooling of the magma (Swanson & Fenn 1986, MacLellan & Trembath 1991).

A second important difference involves the microscopic morphology of phenocryst boundaries. When viewed at high power, phenocryst boundaries in undeformed volcanic rocks tend to be straight and sharp with planar fabric elements in the matrix commonly aligned parallel to the interface on all sides of the phenocryst (Fig. 4h). In deformed rocks, the boundaries, although straight at low magnification, are irregular at high magnification, and foliations typically intersect the interfaces at large angles (Fig. 4g). Further, some matrix quartz grains are optically continuous with the phenocryst, and locally phenocrysts have overgrown the matrix fabric in the outermost 10–20 μm of the crystal. These observations suggest that the quartz phenocrysts have undergone some dynamic recrystallization within several microns of their outermost edge. Several of the most highly-deformed phenocrysts show a continuous transition from phenocryst to recrystallized tail with no distinct boundary (see below). Although 'core and mantle' structures (White 1975) are not ubiquitous, no comparable microstructures have been observed in undeformed volcanic rocks.

Feldspar phenocrysts in both deformed and undeformed volcanic rocks are fractured and offset along crystallographic cleavage planes (Figs. 4c & d). In both types of rocks, fractured feldspar grains can have a 'bookshelf' geometry with either antithetic or synthetic offsets with respect to the direction of bulk shearing. In undeformed volcanic rocks, the fractures are typically infilled with fine-grained, structureless groundmass (Fig. 4d). In deformed rocks, the fragments are typically separated by fibers of metamorphic mica and quartz, typically aligned parallel to the dominant mineral lineation (Fig. 4c).

Matrix microstructures

Both deformational and volcanic processes can produce strong foliations, but important differences exist (Figs. 4e & f). Primary volcanic foliations are defined by flow and compaction structures in the glassy matrix, and by aligned shards, crystals and pumice or other lithic fragments (Schmincke & Swanson 1967). Tectonic foliations are defined by aligned metamorphic muscovite, strained quartz, feldspar and oxides; rootless intrafolial folds are locally present. Both processes can produce asymmetrical tails (shadows) adjacent to phenocrysts. Tails produced during volcanism are defined by flow structures in the glassy matrix (Fig. 4f). They tend to be subtle, can include complex, variably oriented, internal foliations, and are heterogeneously developed even on a single phenocryst. Tectonically produced tails are defined by a greater quartz:mica ratio than matrix material. They have regular, curving internal foliations, and are consistently developed on most phenocrysts in a single sample. Also, phenocrysts in deformed rocks can have mica-rich quarter mats that represent high-strain domains (Hanmer & Passchier 1991). Comparable domains have not been observed in undeformed volcanic rocks.

Deformational fabrics at relatively low metamorphic grades

At low metamorphic grades, it is more difficult to distinguish deformational fabrics from primary volcanic fabrics. Samples of the Proterozoic Red Rock Rhyolite, Arizona (Table 1 and Fig. 1), provide an important type example. They have a variably developed planar fabric that has generally been interpreted as a volcanic flow foliation (K. A. Karlstrom personal communication 1991). The deformational history has been interpreted in terms of foreland-style folding and thrusting (Puls 1986, Doe & Karlstrom 1991), and metamorphic conditions during deformation were approximately 200–400°C, 2.0 kbar (Gillentine *et al.* 1991, Williams 1991b).

Specimens of Red Rock Rhyolite have microstructures characteristic of both the deformed and the undeformed suites (Fig. 5). We suspect that the fine color banding (Fig. 5a) defined by interlayered quartz-dominated and rust-colored, oxide-rich layers represents a primary volcanic flow or compaction fabric. However, we interpret the foliated matrix muscovite, subtle strain shadows (Figs. 5a & b), muscovite-rich quarter mats, recrystallized phenocryst boundaries (Fig. 5d), and folded and recrystallized veinlets (Fig. 5c) to indicate a significant component of ductile deformation, especially given the absence of muscovite in undeformed volcanic rocks. The presence of well-defined muscovite mats in high-strain domains near phenocrysts, and only poorly defined strain shadows in low-strain domains, may indicate that ductile strain was focused at the phenocryst boundaries, but that homogeneous strain in the matrix was generally not high enough to significantly decrease the quartz: mica ratio.

The recognition of ductile deformational microstructures in these low-grade rocks, and the general lack of similar microstructures in other interlayered or associated rock units, has important implications. It suggests that ductile strain may be partitioned into these rocks when other units are still deforming by brittle processes. We suspect that the felsic volcanic rocks may represent important detachment zones, focusing early orogenic, layer-parallel deformation.

Discussion

It is not surprising that similar microstructures are developed during ash-flow tuff emplacement and ductile deformation. Both processes can involve moderate to high-temperature ductile shear. However, significant differences might also be expected because the strain rates are dramatically different. Strain rates for ductile deformation are on the order of $10^{-12}-10^{-18}$ s^{-1} (Pfiffner & Ramsay 1982). Strain rates for emplacement and post-emplacement rheomorphism of volcanic rocks must be many orders of magnitude faster. Ash-flow tuffs are believed to be deposited in a matter of minutes or hours (Smith 1979, Walker 1983), but even assuming that emplacement occurred over a period of a month or more, strain rates would be on the order of 10^{-8}–10^{-7} s^{-1}. At these rapid strain rates, even under near-melting conditions (600–700°C), there may be a greater tendency for quartz phenocrysts to remain undeformed while

Fig. 2. Microstructures in deformed quartz phenocryst-bearing volcanic rocks. (a) Subhedral to euhedral quartz and feldspar phenocrysts in a fine-grained, foliated matrix consisting of quartz, feldspar, muscovite and hematite. (b) Quartz phenocrysts in foliated matrix. Note: (1) compositional layering in the matrix defined by muscovite-rich and muscovite-poor layers and (2) primary volcanic embayments in extinct phenocryst at bottom. (c) Deformational structures associated with phenocrysts. Note: (1) quartz-rich tails on upper right and lower left of phenocrysts, (2) muscovite-rich domains at upper left and lower right, (3) altered and fractured feldspar (upper left), (4) shear bands (bottom center), (5) volcanic embayments in phenocryst (center right). (d) Euhedral quartz phenocryst. Note: (1) fractured and dispersed feldspar phenocryst immediately above the quartz phenocryst, (2) matrix foliation defined by aligned muscovite, hematite and inequant quartz, (3) shear band foliation (upper right to lower left).

Fig. 3. Microstructures in the middle Tertiary, Bloodgood Canyon Tuff, Mogollon Datil volcanic field, New Mexico. (a) Subhedral to euhedral quartz and feldspar phenocrysts in flow-foliated matrix (uncrossed nicols). (b) Quartz and feldspar phenocrysts in flow-foliated matrix (crossed nicols). Foliation is defined by aligned mineral and lithic fragments and by aligned trains of fine opaques, primarily hematite. (c) Euhedral, slightly fractured quartz phenocryst. Note subtle foliation in matrix material. (d) Subhedral, resorbed quartz phenocryst with volcanic embayments.

Fig. 4. Comparison of microstructures in deformed Proterozoic felsic volcanic rocks (left) and Tertiary volcanic rocks (right). (a) & (b) Similar overall appearance of phenocrysts in fine-grained, foliated matrix. Note that foliation in deformed rocks is defined by aligned metamorphic muscovite, hematite, inequant quartz and recrystallized tails on phenocrysts. In undeformed rocks, foliation is defined by mineral fragments, and aligned compositional heterogeneities in the matrix. (c) & (d) Fractured feldspar phenocrysts. In deformed rocks, fragments are separated by aligned quartz and muscovite fibers; in undeformed Tertiary rocks, feldspar fragments are separated by amorphous matrix material. (e) & (f) Subhedral–euhedral quartz phenocrysts with matrix tails (strain shadows). (e) Deformed. Note: (1) systematically curving foliation in tail, (2) grain size becomes progressively finer and quartz : muscovite ratio increases away from phenocryst, (3) muscovite rich 'quarter structure' in high-strain domains (upper left and lower right of phenocryst), (4) phenocryst has some undulose extinction but retains its euhedral form and volcanic embayments. (f) Undeformed. Note: asymmetric tails defined by reoriented matrix material. Tail is well developed at upper right but poorly developed at lower left. Little evidence for high strain domains at upper left and lower right. (g) & (h) Phenocryst–matrix interfaces. (g) Deformed. Irregular, slightly recrystallized interface at high magnification. Foliation intersects interface at a high angle and several matrix grains are optically continuous with phenocryst. (h) Undeformed. Interface is sharp even at high magnification. Near interface, matrix fabric reoriented into parallelism with interface.

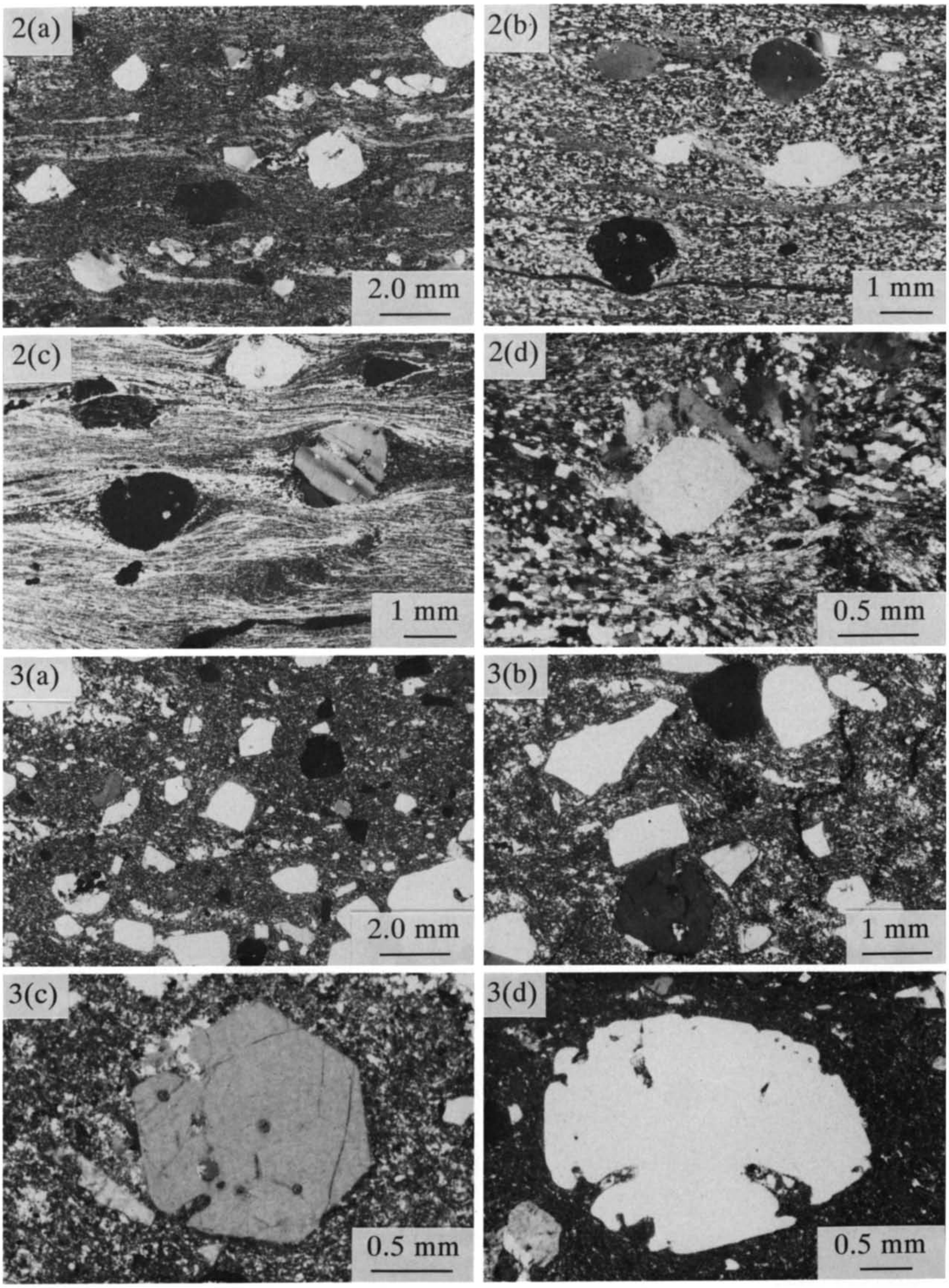

Figs. 2 and 3.

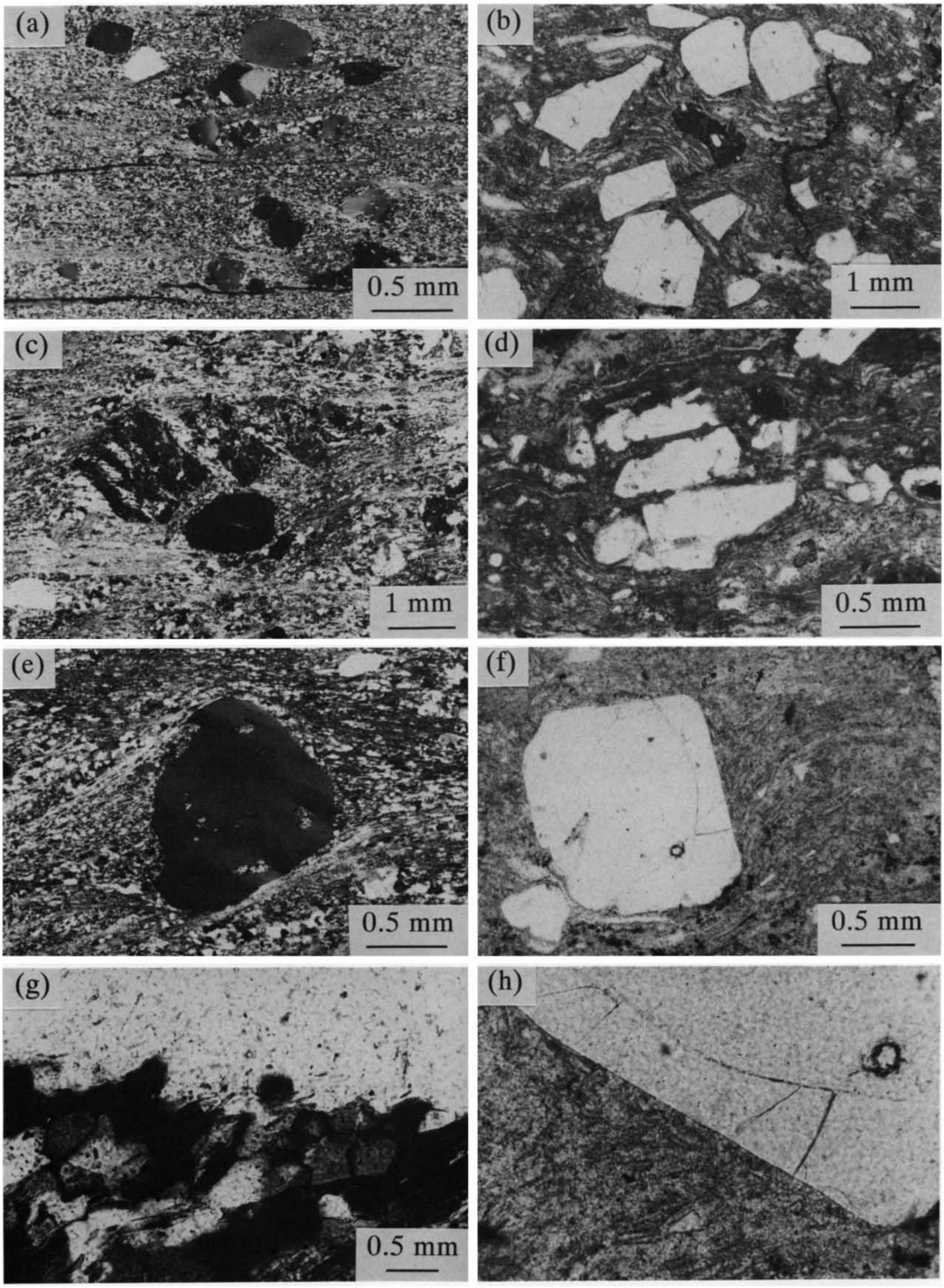

Fig. 4.

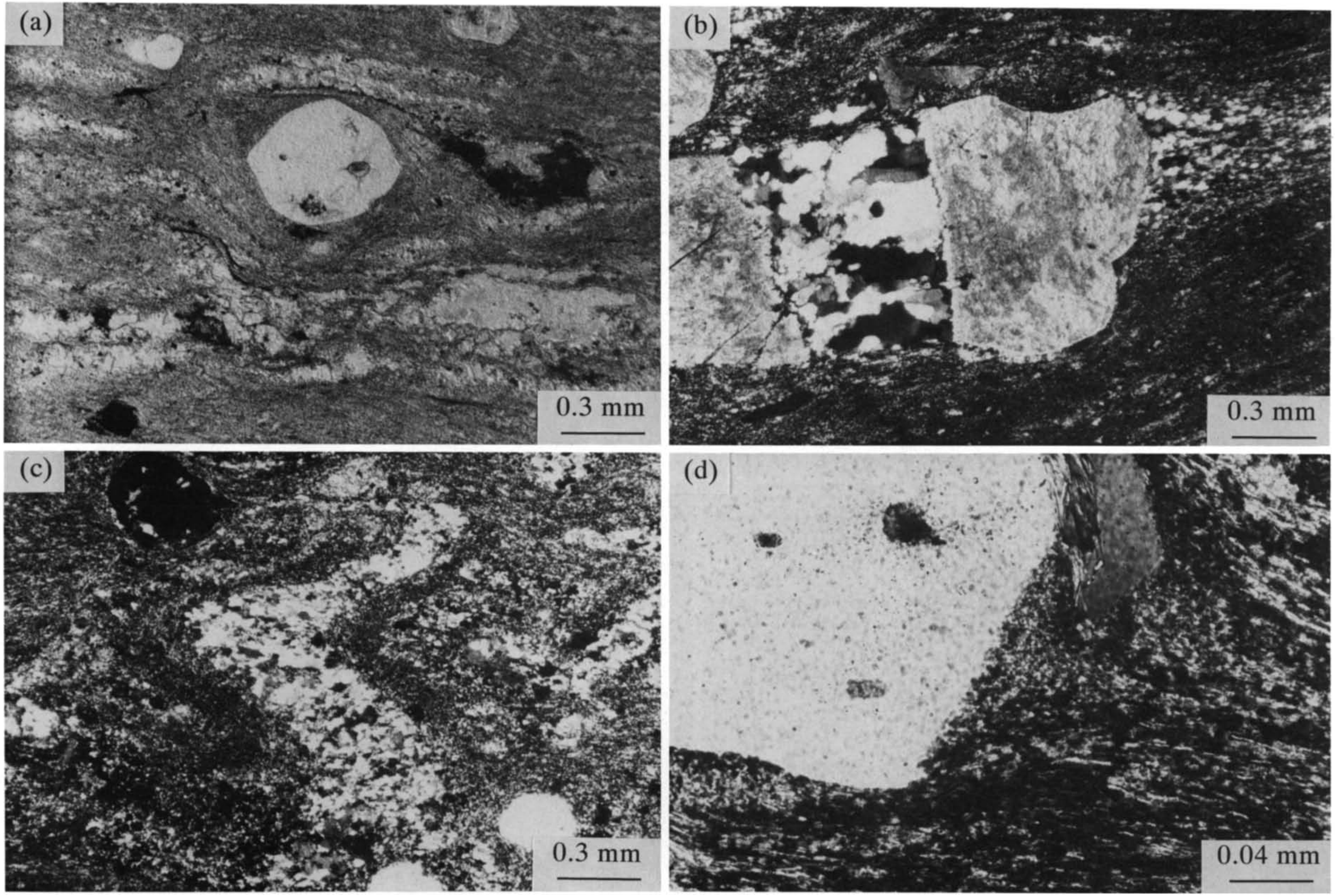

Fig. 5. Microstructures from the Red Rock Rhyolite, Mazatzal Mountains, Arizona (samples provided by K. E. Karlstrom). Metamorphic conditions were approximately 200–400°C, <2 kbar (Gillentine *et al.* 1991). (a) Subhedral–euhedral, undeformed quartz phenocryst in fine-grained quartz, muscovite, hematite matrix. Note well-foliated fine metamorphic muscovite at bottom and left. (b) Fractured K-feldspar phenocryst. Note oriented quartz fibers filling fracture and foliated quartz-rich strain shadow. (c) Folded quartz vein in deformed rhyolite. Vein quartz is strongly recrystallized and foliated, but quartz phenocryst in upper left (at extinction) is undeformed). (d) Phenocryst boundary adjacent to strain shadow. Boundary is irregular and slightly recrystallized. Matrix foliation is defined by aligned muscovite. Foliation curves and weakens toward the strain shadow.

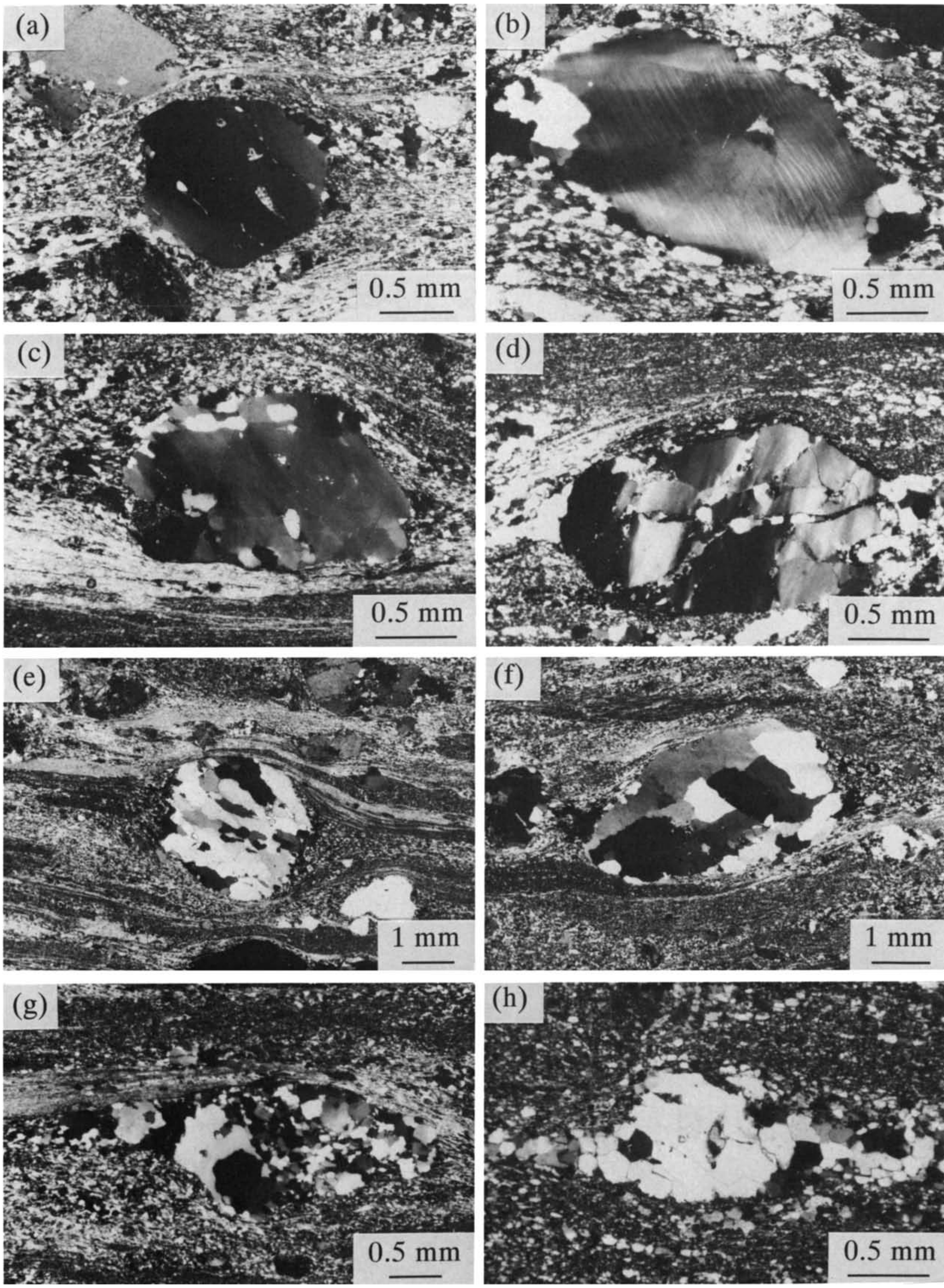

Fig. 6. Progressive deformation of quartz phenocrysts (see discussion in text). Examples come from various specimens and locations but may represent stages in the evolution of a single phenocryst. Metamorphic conditions for all sections were 400–500°C, 3 kbar. All specimens were cut parallel to the stretching lineation and perpendicular to foliation. Crossed nicols.

strain is efficiently partitioned into the hot, fine-grained, volatile-rich matrix.

In attempting to distinguish primary volcanic microstructures from ductile deformational microstructures, the effects of static metamorphism must also be considered. Is it possible to produce microstructures characteristic of ductile deformation by static recrystallization of a primary volcanic fabric? The answer to this question involves understanding the controls on mimetic neocrystallization, the growth of new metamorphic minerals with a preferred orientation dictated by the existing volcanic fabric. Such a process might lead to apparent deformational foliations defined by metamorphic minerals, and it might lead to foliations that curve around phenocrysts. However, mimetic neocrystallization is less likely to produce quartz-rich strain shadows, mica-rich, high-strain domains, deformational substructure in phenocrysts and crystallographic preferred orientation of matrix quartz (see below).

Finally, although it may be readily possible to recognize the effects of ductile deformation in volcanic rocks, the bulk fabric after deformation undoubtedly represents a composite of the original volcanic and superimposed deformational fabrics. Conclusions about the intensity of either process must be made with caution, especially when comparing the intensity of fabrics in volcanic rocks with those in other supracrustal rocks. As discussed below, mildly deformed volcanic rocks can have a porphyroclastic appearance that, in the field, can be strikingly similar to mylonitic rocks, and thus can lead to an overestimation of the magnitude of ductile strain. Conversely, small amounts of ductile deformation may produce a flow-banded appearance in originally unlayered rocks that may lead to misinterpretation of the depositional volcanic environment.

PROGRESSIVE DEFORMATION OF PHENOCRYST-BEARING VOLCANIC ROCKS

The microstructural character of quartz phenocrysts in deformed volcanic rocks varies widely, apparently defining a continuum from euhedral, virtually unstrained phenocrysts to highly strained and recrystallized aggregates or ribbons. The entire spectrum from undeformed to highly deformed phenocrysts can occur in a single thin section, but it is particularly evident when comparing rocks of similar composition from high- or low-strain regimes. Figure 6 shows the typical range of observed microstructures in quartz phenocrysts, organized from undeformed to highly deformed. The photographs come from different rocks in different settings, but all are believed to have been deformed at approximately 400–500°C. To a first approximation, the sequence may represent the evolution of a single phenocryst during progressive deformation.

Quartz crystals with little evidence of deformation are subhedral to euhedral with well-defined crystal faces (Fig. 2). The first evidence of deformation typically involves undulose extinction and deformation bands, inclined approximately 30–50° to the external foliation (Fig. 6a). Less commonly, deformation bands are subparallel to foliation, and deformation lamellae are inclined (Fig. 6b). Local subgrain development and incipient recrystallization have been observed along some crystal faces, particularly adjacent to nearby phenocrysts and along fractures. Interestingly, interaction with nearby phenocrysts appears to concentrate strain even where grains are not actually in contact (Fig. 6a).

At slightly higher strain, subgrain development and rotational recrystallization becomes pronounced on most phenocryst edges (Figs. 6b & c). Although subgrains are developed on all edges, the degree of development is heterogeneous, and no clear relationship has been observed between zones of high matrix strain and zones of increased subgrain development in the phenocrysts. Deformation bands are still present, but subgrains are more pervasively developed across entire crystals (Figs. 6c & d). As noted above, fractures, and rarely embayments, contain fine recrystallized quartz grains that are distinct within the otherwise low-strain cores of phenocrysts (Fig. 6d). This recrystallization may reflect higher strains concentrated near fractures, or it may simply represent coarsening and healing of cataclastic material associated with the fractures (J. Tullis personal communication 1992). From the earliest stages of deformation, relatively large quartz grains (compared to matrix quartz) occur on some phenocryst margins adjacent to strain shadows. Because the phenocryst face is still apparent, these crystals represent new quartz added to the strain shadow area, perhaps as fibers and then recrystallized, rather than dynamically recrystallized phenocryst material (Figs. 6d & e).

With increased deformation, phenocrysts are characterized by extensive subgrain development and rotational recrystallization. Subgrain and recrystallized grain sizes can be homogeneous across the phenocryst (Figs. 6e & f), or they can vary dramatically with separate domains of large and small subgrains in a single phenocryst (Fig. 6g). In addition, neocrystallized grains can be relatively equant (Fig. 6f), or they may have dimensional preferred orientation, subparallel to deformation bands in less deformed phenocrysts (Fig. 6e). Highly recrystallized phenocrysts, now quartz aggregates, are typically elliptical in shape with curved upper and lower surfaces, parallel to the matrix foliation (Figs. 6f & g). However, even highly recrystallized aggregates may retain some of the subhedral to euhedral shape of the original phenocryst (Figs. 6e & f). With increasing deformation, the textural distinction between phenocryst and strain shadow becomes less obvious, and ultimately the recrystallized phenocryst passes continuously into the shadow which itself grades gradually into matrix.

At very high strain, the recrystallized aggregates progress toward smaller grain size and greater flattening parallel to the foliation (Fig. 6g). The ultimate result is the formation of thin lenses or ribbons of polygonal quartz (Fig. 6h). Although in most of the rocks studied we were able to identify the recrystallized phenocrysts even at high strains, it seems possible that some phenocrysts are ultimately homogenized into the deforming matrix. This process may be particularly efficient at high metamorphic grades (see below).

RELATIVE STRENGTH OF QUARTZ PHENOCRYSTS

The most distinctive feature of the deformed volcanic rocks is the strength of the quartz phenocrysts at greenschist to amphibolite facies conditions. In evaluating this apparent strength, two important and perhaps independent observations must be considered. The first is that the quartz phenocrysts are strong relative to most other components in the rocks (other phenocrysts, matrix phases, vein fillings, etc.) and that this relative strength persists, at least in some phenocrysts, throughout the deformational history. The second is that some quartz phenocrysts are strong relative to other quartz phenocrysts. In a typical sample, some quartz phenocrysts have undergone a significant amount of deformation while others remain undeformed. The two observations are discussed separately below.

Controls on the strength of quartz phenocrysts relative to other materials

The apparent strength of quartz phenocrysts relative to matrix has been attributed to "the much greater tendency for fine-grained polymictic aggregates to undergo deformation than large grains, especially where chemical reactions are taking place" (Etheridge & Vernon 1981, Vernon 1986a). Specifically, the partitioning of strain from the phenocrysts to the matrix probably is the result of a number of factors including: (1) the matrix is extremely fine grained, volatile-rich, compositionally heterogeneous and perhaps glassy (at least at the outset of deformation); (2) the quartz phenocrysts are large, relatively dry, single crystals (Etheridge & Vernon 1981); (3) metamorphic reactions may tend to reaction-soften or retard hardening of the matrix during progressive deformation (Etheridge & Vernon 1981); (4) quartz phenocrysts, unlike other phenocrysts and matrix materials, are not softened by metamorphic or alteration reactions; and (5) the quartz phenocrysts may be strengthened (or matrix quartz weakened) by trace elements or other chemical defects that can influence the creep rate (Etheridge & Vernon 1981, Hobbs 1981, Jaoul 1984).

A number of workers have discussed and evaluated the relationship between finite strain and grain size in single-phase (White 1976, Etheridge & Wilkie 1979) and polyphase materials (Etheridge & Vernon 1981). This has been interpreted to reflect the tendency, with decreasing grain size, for an increased role of intergranular deformational mechanisms, such as diffusional creep or grain boundary sliding, relative to intragranular mechanisms, such as dislocation creep (Boullier & Gueguen 1975, Schmid 1976, White 1976). All of the Proterozoic volcanic rocks have extremely fine matrix grain sizes relative to phenocrysts and relative to virtually all other supracrustal rocks. During the early phases of deformation, the fine grain size probably reflects the grain size of the parent volcanic rocks (see Fig. 3). Any volcanic glass still present at the onset of deformation would further enhance the tendency for matrix-dominated deformation. During the later phases of deformation, especially at greenschist to amphibolite conditions, the fine grain size may reflect the ubiquitous presence of dispersed metamorphic minerals (primarily muscovite and hematite) that tend to inhibit grain boundary migration and coarsening (Etheridge & Wilkie 1979, Etheridge & Vernon 1981). As noted above, the matrix of most samples is characterized by well-foliated but generally recrystallized 'equilibrium' microstructures (Vernon 1976) with quartz–quartz grain boundaries commonly pinned against hematite or muscovite crystals. This indicates that some grain boundary migration occurred but that crystals were unable to coarsen significantly. Intergranular muscovite and hematite also may have played a direct role in enhancing the deformability of the matrix; the relatively poorly bonded (001) interfaces would have further facilitated grain boundary diffusion and grain boundary sliding (Etheridge & Vernon 1981).

In contrast to the polycrystalline matrix, quartz phenocrysts are large, single crystals. Internal deformation must occur by fracturing or by lattice slip; volume diffusion could not be significant over these distances. Further, at least at greenschist facies temperatures, lattice slip may be dominated by one slip system $a\{0001\}$ (*a*-glide), which would be possible only in appropriately oriented crystals (Nicolas & Poirier 1976). The differential stress necessary for slip would increase significantly with increasing misorientation of the crystal from this most favorable orientation, but because of the relative ease of deformation of the matrix, differential stresses on the phenocrysts may never be very large.

The strength of quartz during deformation depends on the amount of water in the quartz structure (Griggs & Blacic 1965, Doukhan & Trepied 1985, Ord & Hobbs 1986). The exact mechanism for the weakening remains somewhat unclear, and may depend on the manner in which water is incorporated into quartz (Kronenberg *et al.* 1986, Cordier & Doukhan 1991, Fitzgerald *et al.* 1991). However, regardless of the mechanism, it seems possible that differences in water content may contribute to differences in the behavior of the phenocrysts relative to matrix quartz. As phenocrysts grow in a water-undersaturated magma, water may be efficiently partitioned into the melt; relatively little water may become entrapped in the quartz phenocrysts. At the time of eruption, any remaining magmatic water and surface water associated with the eruption process will become trapped in the fine-grained volcanic matrix and glass. The fine grain size of the matrix may allow further infiltration of fluids during the early stages of deformation, as evidenced by the relatively common clay alteration of feldspar and devitrification of glass. The end result is a rock in which matrix quartz may be significantly more hydrous, and thus more deformable, than the quartz phenocrysts.

Trace elements, in addition to hydrogen, may affect the strength of their host lattice, perhaps by influencing dislocation mobility (Hobbs 1981) or the rate of recovery and recrystallization (Jaoul 1984). For example, Jaoul (1984) suggested that Na may enhance the dislocation glide velocity in quartz, but it may inhibit climb, recovery, and recrystallization processes. We attempted to detect trace components in phenocryst and matrix quartz from several samples using broad beam (~10 μm) and focused beam (~2 μm) electron microprobe analyses. No trace elements (not even Ti or Na) were found to be present above the approximately 0.1–0.2 wt% detection limits. Although it is possible that quartz phenocrysts may be somewhat strengthened, or matrix quartz weakened, by the presence of one or more trace elements, this effect is suspected to be minor compared to the influence of other factors such as hydrolysis (see Jaoul 1984).

Feldspar phenocrysts are deformed in many of the volcanic rocks, but the deformation generally involves chemical alteration or fracturing along crystallographic cleavage planes. These observations emphasize several important factors about the strength of the quartz phenocrysts. First, at low and medium metamorphic grades, quartz phenocrysts do not appear to be involved in any alteration or chemical reactions, particularly in rocks of such quartz-rich bulk compositions. Thus, deformation is not aided by reaction effects. Second, quartz has no crystallographic cleavage and most phenocrysts are largely unfractured, denying fluid access to the inner parts of the crystals. Stresses during deformation were apparently sufficient to break feldspar grains along cleavage planes, but they were generally not large enough to produce fractures in the more isotropic quartz structure.

Heterogeneous deformational behavior of quartz phenocrysts

Within a single specimen, quartz phenocrysts commonly range from undeformed to highly recrystallized. Although the extent of deformation probably varies with local finite strain and strain rate, no straightforward relationship is apparent. Instead, it seems that the degree of deformation of quartz phenocrysts probably reflects a combination of factors, the effects of which are difficult to predict in any one sample. These include: (1) the geometry of strain partitioning; (2) access of fluids provided by fractures and embayments; (3) phenocryst interactions; (4) crystallographic orientation; and (5) compositional or structural heterogeneities. Each of these is briefly discussed below.

The natural material heterogeneity of most rocks, from the grain scale to the continent scale, leads to anastomosing domains of high and low strain, even during a relatively homogeneous bulk deformation (Bell 1981). The presence of unstrained phenocrysts in highly-strained matrix indicates an efficient strain partitioning at the phenocryst scale. The presence of compositional layering, grain size variations, *S–C* fabric and variations in the overall microstructural character of the rocks suggests that strain was also heterogeneous at the scale of the thin section and larger. Some of the variation in the degree of deformation of quartz phenocrysts probably reflects this thin-section-scale partitioning of strain and strain rate, although as noted no correlation with visible high-strain domains is apparent.

The ease with which water can reach the internal parts of quartz phenocrysts may be important in influencing the strength of some quartz phenocrysts relative to others. The presence of a bimodal population of highly deformed and undeformed phenocrysts in some specimens suggests that phenocrysts may deform more easily once they begin to deform, i.e. they may strain soften (Poirier 1985). Microfractures formed during the volcanic eruption or during the early phases of deformation may allow water to gain access to the interior of the phenocrysts, thereby facilitating hydrolytic weakening and further deformation. If so, progressive deformation may tend to preferentially remove fractured or imperfect quartz phenocrysts and preserve the least fractured phenocrysts. As with microfractures, embayments might be expected to allow water to access the interior of the phenocrysts. However, we have observed no tendency for the preferential removal of embayment-rich phenocrysts during deformation.

Mechanical interaction between phenocrysts may also be important in initiating deformation in an otherwise undeformed phenocryst. Examples have been noted in which internal deformation and recrystallization are localized at the point of contact between two adjacent phenocrysts (Figs. 3a and 4a). The phenocrysts apparently behave as stress risers focusing stress at the margin of one or both phenocrysts and interrupting the pattern of strain partitioning around the crystals. Commonly, deformation is induced in only one of the pair, further emphasizing the strength contrasts between the phenocrysts.

The orientation of the quartz phenocrysts with respect to the stress field may be an additional cause of strength heterogeneity, and thus strain heterogeneity among the phenocrysts. Such strength variation with orientation has been demonstrated experimentally in synthetic quartz (Linker *et al.* 1984) and in experimentally deformed natural quartz mylonites (Ralser *et al.* 1991). As a test, quartz phenocrysts from several samples were qualitatively divided into two populations, relatively strained (distinctly undulose) and unstrained (little or no undulose extinction). The orientations of quartz *c*-axes of both populations and matrix quartz grains were measured on a universal stage (Fig. 7). Plots of strained quartz and matrix quartz are distinctly non-random, suggesting that crystal plastic processes were active. The distributions generally show a symmetrical distribution of *c*-axes, interpreted to result from dominantly coaxial strain (Schmid & Casey 1986). Plots of less-deformed

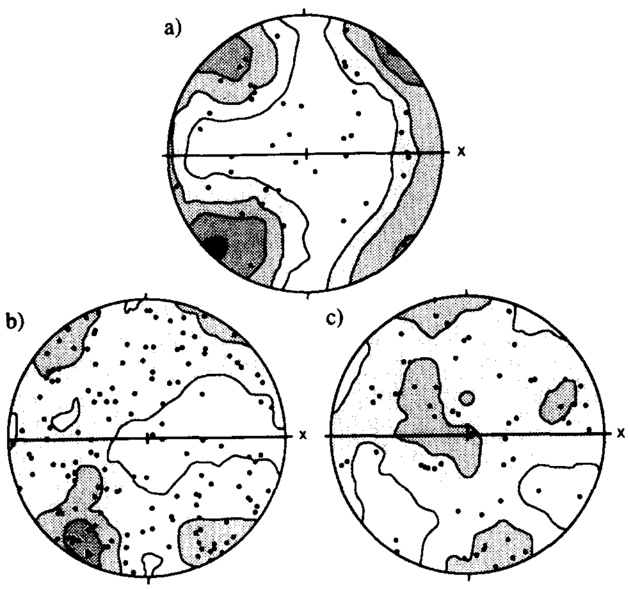

Fig. 7. Equal-area quartz c-axis plots from selected specimens. For all plots, foliation is horizontal. (a) Shylock zone, Hieroglyphic Mountains, Arizona. Contours represent matrix quartz (N = 106). Points represent strained (undulose extinction) and unstrained quartz phenocrysts (N=48). (b) Shylock shear zone, Black Canyon City, Arizona. Points and contours represent strained phenocrysts (N = 154). (c) Same sample as (b) showing unstrained phenocrysts (N = 65). Kamb contour interval = 2 σ.

phenocrysts from the same specimen lack concentrations around the maxima for the strained grains. Instead, c-axes tend to be concentrated near the Y-axis of finite strain. These phenocrysts have their basal planes in the X–Z plane of finite strain, an orientation that is unfavorable for a-slip during pure shear deformation (Fig. 7). The tendency for deformed phenocrysts to have orientations favorable for strain and for relatively undeformed phenocrysts to have less favorable orientations suggests that crystallographic orientation indeed has an influence on the relative strength of the quartz phenocrysts. Further, the data suggest that rotation of phenocrysts is minimal during deformation or else the favorable and unfavorable orientations could not be maintained.

Finally, some variation in the degree of deformation of quartz phenocrysts may be controlled by original heterogeneities in composition or structure of the quartz crystals. It seems possible that subtle variations in fluid content, fracture density, dislocation or vacancy density, or trace element content may exist among quartz phenocrysts in an evolving magmatic system. If the various populations become mixed, either in the magma chamber or during eruption, the compositional variations may lead to subtle variations in strength.

Speculations: relative strength of quartz phenocrysts at high metamorphic grade

Upper amphibolite or granulite facies supracrustal rocks are not common in the American Southwest, but they are present near several syn-tectonic plutons and in the Mojave Province of northwestern Arizona and California (J. L. Anderson 1989, Williams 1991b). Quartz phenocryst-bearing volcanic rocks are rare or absent in these regions even though the supracrustal sequences are similar to those in the lower-grade regions. Further, although some examples exist (Stanton 1976, Vernon 1986a), descriptions of abundant phenocryst-bearing felsic volcanic rocks from other granulite facies terranes appear to be rare in the geologic literature.

The apparent lack of 'quartz-eye' rhyolites at high metamorphic grade may reflect a change in the deformational behavior of felsic volcanic rocks. With increasing metamorphic grade and diffusion rate, the matrix grain size would increase (Spry 1969), and the distinction between phenocrysts and matrix diminish. Further, with the breakdown of muscovite, in most rocks at the second sillimanite isograd (Evans & Guidotti 1966), these biotite-poor rocks will be increasingly anhydrous and mechanical differences between phenocrysts and matrix will be further diminished. Thus, at high metamorphic grades, strain may be more successfully partitioned into the phenocrysts, leading to their eventual recrystallization. Assuming that the original feldspar grains were fractured or altered at lower grades, the end result is a medium- to coarse-grained equigranular quartzofeldspathic rock, common in granulite facies terranes.

STRAIN ANALYSIS

Qualitative estimates based on outcrop appearance

Felsic volcanic rocks have a distinctive outcrop appearance relative to most other supracrustal rocks. In the southwestern United States, they are associated with a variety of schists and gneisses, all of which have a relatively coarse-grained, granoblastic texture that tends to be insensitive to the magnitude or nature of finite strain. In contrast, felsic volcanic rocks are extremely fine grained, with well-developed microbanding and a complex array of microstructures, including intrafolial folds, phenocrysts–porphyroclasts with recrystallized tails, and lenses and stringers of quartz, carbonate or oxides. Together these microstructures produce an outcrop appearance that is reminiscent of highly deformed mylonites, especially mylonitized granitoids. The main evidence contradicting this interpretation is the presence of euhedral quartz phenocrysts; quartz crystals are rarely preserved in mylonitized granitoids (Vernon 1986a).

The mylonitic appearance of deformed felsic volcanic rocks may lead to erroneous conclusions about their deformational history compared to associated rock units. In some instances, workers may conclude that they represent domains of high strain rather than lithologically distinct domains. In some regions, this may be a reasonable interpretation. Because of their originally fine grain size and possibly glassy character, these rocks may tend to localize early layer-parallel deformations. However, we urge extreme caution in evaluating the magnitude of finite strain in deformed volcanic rocks. Most of the characteristics that give the rocks their mylonitic appearance are also characteristic of undeformed volcanic rocks. One must also be cautious in comparing the magnitude of finite strain between outcrops or specimens of deformed rhyolite. During progressive deformation, phenocrysts are progressively deformed and recrystallized, but because of the original variability in the density of phenocrysts and the extreme heterogeneity with which phenocrysts are deformed, no quantifiable relationship is apparent between the character or concentration of phenocrysts and the magnitude of finite strain.

Fry analysis of phenocryst-bearing volcanic rocks

We have attempted to describe the finite strain state in deformed and undeformed volcanic rocks using the center-to-center ('Fry') method (Fry 1979, Ramsay & Huber 1983) on quartz phenocrysts. Typical samples of felsic volcanic rocks have comparatively few phenocrysts for optimal center-to-center analysis. Most thin sections of slabs have fewer than 100 phenocrysts, and preliminary data suggest that several hundred points or more may be desirable (Crespi 1986). However, even when fewer points are available, the poorly-defined ellipses are generally compatible with deformational fabrics, and thus useful information can be gained about the orientation, if not the magnitude, of finite strain.

Results of center-to-center analyses on undeformed volcanic rocks were presented by Seaman & Williams (1992). Analyses carried out on sections parallel to the plane of compaction yielded ellipses roughly parallel to the volcanic flow direction, and therefore the technique was suggested to be useful for flow direction determination in homogeneous volcanic rocks (Seaman & Williams 1992). Results on sections cut normal to layering and parallel to lineation were difficult to interpret. Some ellipses have long axes parallel to the layering (volcanic foliation), but others are nearly normal to layering. Seaman & Williams (1992) suggested that these ellipses reflect heterogeneity in the original distribution of phenocrysts caused by sorting, flow differentiation, compaction and fragmentation. For comparison, center-to-center analyses were carried out on 14 deformed samples. The results are similar to those from undeformed rocks. Sections or slabs cut parallel to the main foliation yielded ellipses with their long axes parallel to the principal mineral lineation. In sections oriented normal to foliation, some ellipses are parallel to the foliation, but others are oriented at various angles to it. Several enigmatic, non-elliptical plots were also produced.

Several tentative conclusions can be drawn from these analyses. (1) Strain analyses carried out in the X–Z plane of strain (lineation-parallel and foliation normal) yield complicated results which seem to prohibit comparison, although a larger percentage of the deformed rocks have ellipses parallel to the foliation plane. If the original distributions were similar, this suggests that the flattening component of ductile strain may have been large enough to mask the original heterogeneities in the phenocryst distribution. (2) Analyses carried out in the X–Y plane of strain are generally straightforward; ellipses are parallel to the mineral lineation or, in undeformed rocks, the transport lineation. Unfortunately the ellipticities are small, and no direct relationship was observed with the magnitude of finite strain. (3) Contrary to the results of Knight *et al.* (1986) on undeformed tuffs, no relationship was observed between the direction of inclination of the strain ellipse and the direction of shear or volcanic flow. In the rocks investigated here, asymmetrical fabric elements are significantly more reliable and interpretable as kinematic indicators (see below).

Kinematic indicators and kinematic analysis in deformed volcanic rocks

Quartz phenocryst-bearing volcanic rocks can be extremely useful for kinematic analysis of deformed supracrustal sequences. Several types of kinematic indicators are present, the most important of which are asymmetrical strain shadows and recrystallized tails on quartz phenocrysts. As discussed above, primary and secondary asymmetrical structures are generally distinguishable except in some low-grade samples. Although sigma and delta type porphyroclast tails can be difficult to distinguish in some rocks (Hanmer & Passchier 1991), the tails in deformed volcanic rocks are typically straight and long (several times longer than the width of the phenocryst, and are abundantly developed. Under these circumstances, they can be more confidently interpreted as sigma-type geometries. Also, locally developed S–C fabrics and C' ('shear band') foliations add further confidence to the kinematic interpretations drawn from the asymmetrical structures.

For several reasons, the quartz phenocrysts may represent a unique type of porphyroclast for structural and kinematic analysis. First, the quartz phenocrysts apparently behave as porphyroclasts throughout the entire deformational history of the rocks. Unlike metamorphic rocks or tectonized plutonic rocks, the structural character of the volcanic rocks, with large strong crystals in a fine-grained deformable matrix, is established before the onset of deformation. Metamorphic porphyroblasts and porphyroclasts in deformed plutonic rocks may not develop until the later parts of the deformational history. In many regions, early structural events involve some of the most significant translations, and volcanic rocks have the potential to preserve these phases of the kinematic history. Secondly, many schistose metamorphic rocks undergo a significant amount of recrystallization and grain-size coarsening during the later phases of deformation. This recrystallization can obscure kinematic information preserved from the earlier events, and again may emphasize the effects of the latest deformation. Because the deformed volcanic rocks are dominated by equigranular quartz and feldspar, the effects of recrystallization and coarsening are rather minimal, underscoring their possible importance as kinematic indicators for the earlier parts of the history. The final sections of this paper provide two examples in which deformed quartz-eye rhyolites have yielded important and perhaps unique kinematic information.

Early shearing events, Tusas Mountains, New Mexico. The geometry of large-scale structures in the Tusas Mountains and throughout northern New Mexico suggests N-verging ductile thrusting and crustal shortening (Fig. 8a) (Bauer 1988, Williams 1990). However, most rocks are strongly recrystallized, and kinematic indicators documenting the compressional tectonic events have not been widely recognized (Williams 1990, 1991a). Instead, kinematic indicators in some quartzites and schists suggest 'S-directed', extensional tectonism (Grambling *et al.* 1989). Many workers agree that the general lack of kinematic indicators reflects the fact that amphibolite facies metamorphism occurred late in the deformational history. However, the contrasting nature of large-scale and small-scale kinematic information has contributed to ongoing controversy over the tectonic setting and tectonic history of these Proterozoic rocks, particularly the relative importance of extensional vs compressional processes.

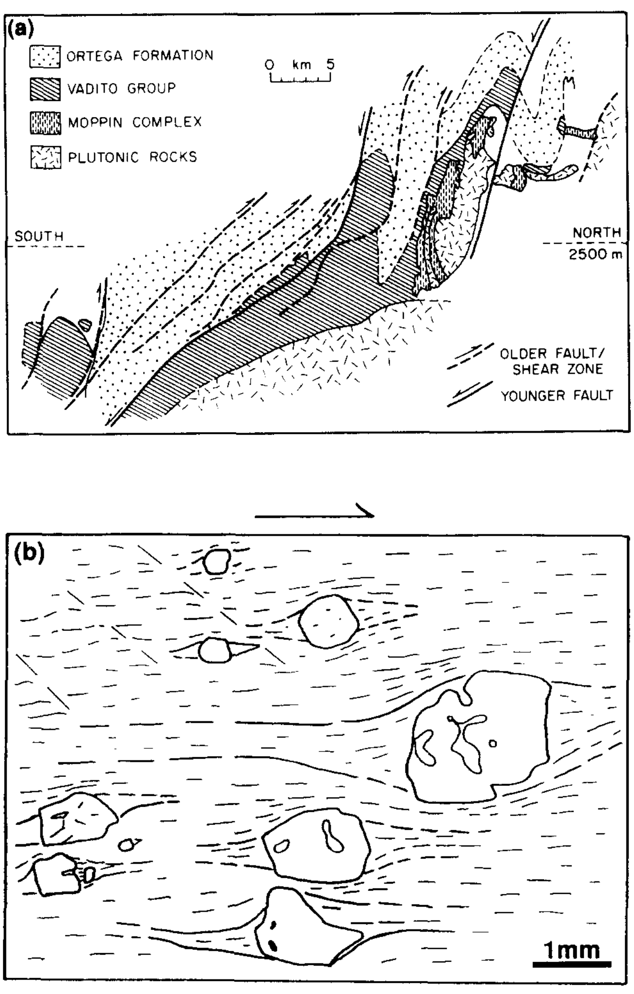

Fig. 8. Kinematic analysis of Proterozoic rocks, Tusas Mountains, New Mexico. (a) Down-plunge projection of large-scale structural relationships (modified from Williams 1991). Note the N-vergence of most large-scale structural ductile faults, but several major structures are interpreted to have been reactivated as normal faults/shears. (b) Thin section sketch of quartz phenocryst-bearing schist from Burned Mountain Formation, northern Tusas Mountains. Asymmetry of strain shadow tails suggests top to right, N-verging shear, consistent with inferred early compressional events.

Quartz phenocryst-bearing volcanic rocks in the Tusas Mountains preserve evidence for the early N-verging event(s) (Williams 1990). Kinematic indicators are particularly well developed in the Burned Mountain Formation of the Vadito Group (Barker 1958, Bauer & Williams 1989) in the northern part of the range. In these rocks, asymmetrical recrystallized tails on quartz phenocrysts and local shear bands document N-verging shear (Fig. 8b). Several samples may also preserve subtle evidence for a later S-verging event. Asymmetrical, S-verging microfolds of the dominant schistosity and of quartz-rich tails on phenocrysts have been recognized in several samples. These observations are consistent with a geologic history involving early N-verging, compressional motion and later, S-verging, extensional motion. The fact that early kinematic indicators are well preserved in felsic volcanic rocks and are virtually absent in other rock types reflects the fact that the volcanic rocks were not strongly affected by the late-stage metamorphism and static recrystallization. To a lesser degree, it also reflects the fact that the later phases of deformation were apparently partitioned away from the volcanic units into the more schistose rocks. We suspect that variations in the mechanical properties of the units with temperature favor deformation of the rhyolites during the lower-grade parts of the prograde history, and favor deformation of the schistose units at amphibolite facies conditions (i.e. during the S-verging events).

Two phases of shearing, Hieroglyphic Mountains, central Arizona. The Hieroglyphic Mountains are located at the southeast margin of the Early Proterozoic Yavapai province (Karlstrom & Bowring 1991, Burr 1991, 1992) within central Arizona's transition zone (Figs. 1 and 9). Two nearly orthogonal foliations are heterogeneously developed throughout the Yavapai province (Karlstrom & Bowring 1991). They are interpreted to represent two major phases of orogenic shortening, but few data exist on the kinematics of the earlier event (Darrach *et al.* 1991, Karlstrom & Bowring 1991). In the Hieroglyphic Mountains, the first phase of deformation is preserved as a foliation subparallel to bedding and a well-developed mineral lineation. In many areas, this phase 1 fabric is strongly overprinted by second-phase deformation. However, some phenocryst-bearing volcanic rocks and sediments are only weakly deformed by the later phase, and asymmetrical tails on quartz phenocrysts indicate an east-over-west sense of shear. This supports the interpretation that the early fabric represents a phase of NW-directed, bedding-parallel thrusting, rarely preserved in other areas within the Yavapai province (Burr 1991, Karlstrom & Bowring 1991). The second phase of deformation is characterized by a NE-striking, steeply dipping cleavage and shear zones with steeply plunging mineral lineations. Asymmetrical tails on quartz phenocrysts in phase 2-dominated domains show a northwest-over-southeast

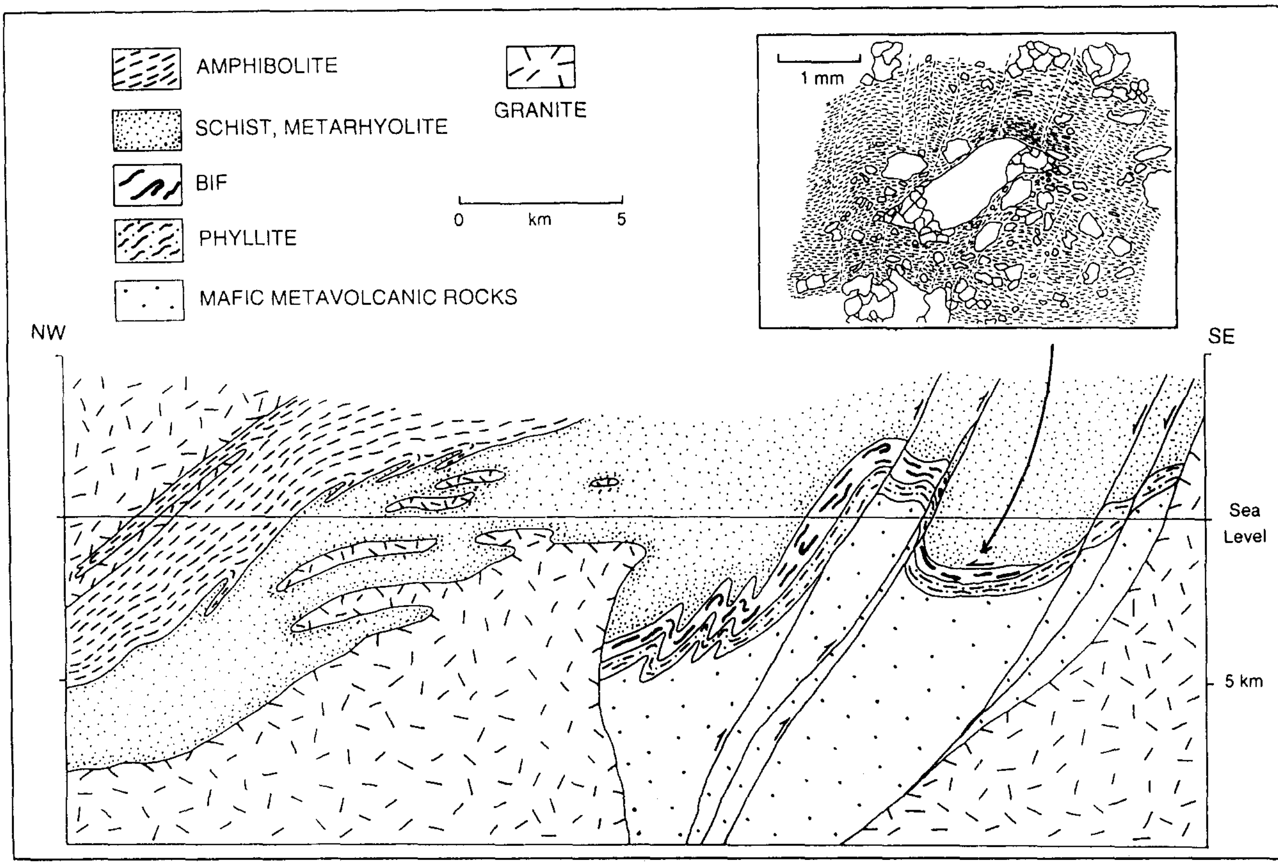

Fig. 9. Diagrammatic cross-section of Early Proterozoic rocks in the Hieroglyphic Mountains, central Arizona (Fig. 1, area 8). Zone of northwest-side-up faults corresponds to the Shylock shear zone. Sketch of quartz phenocryst with asymmetric tails depicts phase 1 southeast-over-northwest (top-to-the-left) shear fabric crenulated and cut by weakly developed phase 2 cleavage. Dashes represent matrix muscovite. Phase 1 fabrics in the Shylock zone are strongly overprinted and transposed, and quartz phenocrysts in domains of high phase 2 strain display northwest-side-up kinematics.

sense of movement that is consistent with other kinematic indicators.

Thus, in the Hieroglyphic Mountains, quartz phenocryst-bearing rocks document the kinematics of both major deformational phases. However, although some felsic volcanic rocks have both foliations, most have one strong foliation that can be classified only by its orientation and field relationships. In many domains, evidence for the early fabric has been completely obliterated by second-phase transposition, yet quartz eyes are preserved through both deformations.

Acknowledgements—This research was partially supported by NSF grant EAR-8916494 (to M. L. Williams). Official review comments were provided by R. H. Vernon, P. Karabinos, S. Woital and an anonymous reviewer. Unofficial, but equally careful and critical, comments were provided by J. Tullis, D. Janey and S. J. Seaman. The paper was vastly improved by the insightful comments and painstaking editorial suggestions of these reviewers. Helpful discussions with P. Bauer, J. Grambling, K. Karlstrom, V. Peterson and D. Wise are also much appreciated.

REFERENCES

Anderson, C. A. & Blacet, P. M. 1972. Precambrian geology of the northern Bradshaw Mountains, Yavapai County, Arizona. *Bull. U.S. geol. Surv.* **1336**.

Anderson, J. L. 1989. Proterozoic anorogenic granites of the southwestern United States. In: *Geologic Evolution of Arizona* (edited by Jenney, J. P. & Reynolds, S. J.). *Arizona geol. Soc. Digest* **17**, 211–238.

1Anderson, P. 1989. Stratigraphic framework, volcanic-plutonic evolution, and vertical deformation in the Proterozoic volcanic belts of central Arizona. In: *Geologic Evolution of Arizona* (edited by Jenney, J. P. & Reynolds, S. J.). *Arizona geol. Soc. Digest* **17**, 57–148.

Barker, F. 1958. Precambrian and Tertiary geology of Las Tablas quadrangle, New Mexico. *Bull. New Mexico Bur. Mines & Miner. Resourc.* **45**.

Bauer, P. W. 1983. Geology of the Precambrian rocks of the southern Manzano Mountains, New Mexico. Unpublished M.S. thesis, University of New Mexico.

Bauer, P. W. 1988. Precambrian geology of the Picuris Range, north-central New Mexico. *New Mexico Bur. Mines & Miner. Resourc. Open-file Rep.* **325**.

Bauer, P. W. & Williams, M. L. 1989. Stratigraphic nomenclature of Proterozoic rocks, northern New Mexico—revisions, redefinitions, and formalization. *New Mexico Geol.* **11**, 45–52.

Bell, T. H. 1981. Foliation development—the contribution, geometry and significance of progressive bulk inhomogeneous shortening. *Tectonophysics* **75**, 273–296.

Bingler, E. C. 1965. Precambrian geology of La Madera quadrangle, Rio Arriba County, New Mexico. *Bull. New Mexico Bur. Mines & Miner. Resourc.* **80**.

Boullier, A. M. & Gueguen, Y. 1975. SP-mylonites: origin of some mylonites by superplastic flow. *Contr. Miner. Petrol.* **50**, 93–104.

Burr, J. L. 1991. Proterozoic stratigraphy and structural geology of the Hieroglyphic Mountains, central Arizona. *Spec. Pap. Arizona geol. Soc.* **19**, 117–133.

Burr, J. L. 1992.Early Proterozoic structural geology, metamorphism, and effects of pluton emplacement, southern Big Bug tectonic block, Hieroglyphic Mountains, central Arizona. Unpublished Ph.D. dissertation, University of Massachusetts–Amherst.

Chaplin, C. E. & Lowell, F. R. 1979. Primary and secondary flow structures in ash-flow tuffs of the Gribbles Run paleovalley, central

Colorado. In: *Ash Flow Tuffs* (edited by Chapin, C. E. & Elston, W. E.). *Spec. Pap. geol. Soc. Am.* **180**, 137–154.

Conway, C. M. 1976. Petrology, structure, and evolution of a Precambrian volcanic and plutonic complex, Tonto Basin, Gila County, Arizona. Unpublished Ph.D. dissertation, California Institute of Technology.

Conway, C. M. & Silver, L. T. 1989. Early Proterozoic rocks (1710–1615 Ma) in central to southeastern Arizona. In: *Geologic Evolution of Arizona* (edited by Jenney, J. P. & Reynolds, S. J.). *Arizona geol. Soc. Digest* **17**, 165–186.

Cordier, P. & Doukhan, J. C. 1991. Water speciation in quartz: A near infrared study. *Am. Mineral.* **76**, 361–369.

Crespi, J. M. 1986. Some guidelines for the practical application of Fry's method of strain analysis. *J. Struct. Geol.* **8**, 799–808.

Darrach, M. E. 1988. A kinematic and geometric structural analysis of an Early Proterozoic crustal-scale shear zone: The evolution of the Shylock fault zone, central Arizona. Unpublished M.S. thesis, Northern Arizona University.

Darrach, M. E., Karlstrom, K. E., Williams, M. L. & Argenbright, D. M. 1991. Progressive deformation in the Early Proterozoic Shylock shear zone, central Arizona. In: *Proterozoic Geology and Ore Deposits of Arizona* (edited by Karlstrom, K. E.). *Arizona geol. Soc. Digest* **19**, 97–116.

DeRosen-Spence, A. F. & Spence, C. D. 1977. "Quartz-eye" bearing porphyroidal rocks and volcanogenic massive sulfide deposits—a discussion. *Econ. Geol.* **72**, 313–314.

Doe, M. & Karlstrom, K. E. 1991. Structural geology of an Early Proterozoic foreland thrust belt, Mazatzal Mountains, Arizona. In: *Proterozoic Geology and Ore Deposits of Arizona* (edited by Karlstrom, K. E.). *Arizona geol. Soc. Digest* **19**, 181–192.

Doukhan, J. C. & Trepied, L. 1985. Plastic deformation of quartz single crystals. *Bull. Mineral.* **108** 97–123.

Elston, W. E. 1984. Mid-Tertiary ash flow tuff cauldrons, southwestern New Mexico. *J. geophys. Res.* **89**, 8733–8750.

Elston, W. E. & Smith, E. I. 1970. Determination of flow direction of rhyolitic ash flow-tuff from fluidal textures. *Bull. geol. Soc. Am.* **81**, 3393–3406.

Etheridge, M. A. & Vernon, R. H. 1981. A deformed polymictic conglomerate—the influence of grain size and composition on the mechanism and rate of deformation. *Tectonophysics* **79**, 237–254.

Etheridge, M. A. & Wilkie, J. C. 1979. Grain size reduction, grain boundary sliding and the flow strength of mylonites. In: *Microstructural Processes During Deformation and Metamorphism* (edited by Bell, T. H. & Vernon, R. H.). *Tectonophysics* **58**, 159–178.

Evans, B. W. & Guidotti, C. V. 1966. The sillimanite–potash feldspar isograd in western Maine, USA. *Contr. Miner. Petrol.* **12**, 25–62.

Fitzgerald, J. D., Boland, J. N., McLaren, A. C., Ord, A. & Hobbs, B. E. 1991. Microstructures in water-weakened single crystals of quartz. *J. geophys. Res.* **96**, 2139–2155.

Frater, K. M. 1983. Effects of metasomatism and development of quartz eyes in intrusive and extrusive rocks at Golden Grove Cu–Zn deposit, Western Australia. *Trans. Instn. Min. Metall.* **92**, B121–B131.

Fry, N. 1979. Random point distributions and strain measurement in rocks. *Tectonophysics* **60**, 806–807.

Gillentine, J., Karlstrom, K. E., Parnell, R. A., Jr & Puls, D. 1991. Constraints on temperatures of Proterozoic metamorphism in low grade rocks of central Arizona. In: *Proterozoic Geology and Ore Deposits of Arizona* (edited by Karlstrom, K. E.). *Arizona geol. Soc. Digest* **19**, 165–180.

Goodspeed, G. E. 1937. Development of quartz porphyroblasts in siliceous hornfels. *Am. Mineral.* **22**, 133–138.

Grambling, J. A., Williams, M. L., Smith, R. F. & Mawer, C. K. 1989. The role of crustal extension in the metamorphism of Proterozoic rocks in northern New Mexico. In: *Proterozoic Geology of the Southern Rocky Mountains* (edited by Grambling, J. A. & Tewksbury, B. J.). *Spec. Pap. geol. Soc. Am.* **235**, 87–110.

Gresens, R. L. & Stensrud, H. L. 1974. Recognition of more metarhyolite occurrences in northern New Mexico and a possible Precambrian stratigraphy. *Mountain Geologist* **11**, 109–124.

Griggs, D. T. & Blacic, J. D. 1965. Quartz: anomalous weakness of synthetic crystals. *Science* **147**, 292–295.

Hanmer, S. & Passchier, C. 1991. Shear sense indicators: a review. *Geol. Surv. Pap. Can.* **90-17**.

Hobbs, B. E. 1981. The influence of metamorphic environment upon the deformation of minerals. *Tectonophysics* **78**, 335–383.

Hoffman, P. F. 1988. United Plates of America: birth of a craton. *Annu. Rev. Earth & Planet. Sci.* **16**, 543–603.

Hopwood, T. P. 1976. "Quartz-eye"-bearing porphyroidal rocks and volcanogenic massive sulfide deposits. *Econ. Geol.* **71**, 589–612.

Hopwood, T. P. 1977. "Quartz-eye"-bearing porphyroidal rocks and volcanogenic massive sulfide deposits—a reply. *Econ. Geol.* **72**, 701–703.

Jaoul, O. 1984. Sodium weakening of Heavitree quartzite: preliminary results. *J. geophys. Res.* **89**, 4271–4280.

Jerome, S. E. 1956. Reconnaissance geologic study of the Black Canyon schist belt, Bradshaw Mountains, Yavapai and Maracopa Counties, Arizona. Unpublished Ph.D. thesis, University of Utah.

Karlstrom, K. E. & Bowring, S. A. 1988. Early Proterozoic assembly of tectonostratigraphic terranes in southwestern North America. *J. Geol.* **96**, 561–576.

Karlstrom, K. E. & Bowing, S. A. 1991. Styles and timing of Early Proterozoic deformation in Arizona. In: *Proterozoic Geology and Ore Deposits of Arizona* (edited by Karlstrom, K. E.). *Arizona geol. Soc. Digest* **19**, 1–10.

Karlstrom, K. E., Doe, M. F., Wessels, R. L., Bowring, S. A., Dann, J. C. & Williams, M. L. 1990. Juxtaposition of Proterozoic crustal blocks: 1.65–1.60 Ga Mazatzal orogeny. In: *Geological Excursions Through the Sonoran Desert Region, Arizona and Sonora* (edited by Gehrels, G. E. & Spencer, J. E.). *Spec. Pap. Arizona geol. Surv.* **7**, 114–123.

Knight, M. D., Walker, G. P. L., Ellwood, B. B., Diehl, J. F. 1986. Stratigraphy, paleomagnetism, and magnetic fabric of the Toba Tuffs: constraints on the sources and eruptive styles. *J. geophys. Res.* **91**, 10,355–10,382.

Kronenberg, A. K., Kirby, S. H., Aines, R. D. & Rossman, G. R. 1986. Solubility and diffusional uptake of hydrogen in quartz at high water pressures: Implications for hydrolytic weakening. *J. geophys. Res.* **91**, 12,723–12,744.

Linker, K. F., Kirby, S. H., Ord, A. & Christie, J. M. 1984. Effects of compression direction on the plasticity and rheology of hydrolytically weakened synthetic quartz crystals at atmospheric pressure. *J. geophys. Res.* **89**, 424–4255.

MacLellan, E. H. & Trembath, L. T. 1991. The role of quartz crystallization in the development and preservation of igneous texture in granitic rocks: Experimental evidence at 1 kbar. *Am. Mineral.* **76**, 1291–1305.

Nicolas, A. & Poirier, J. P. 1976. *Crystalline Plasticity and Solid-state Flow in Metamorphic Rocks*. Wiley Interscience, London.

Ord, A. & Hobbs, B. E. 1986. Experimental control of the water weakening effect in quartz. In: *Mineral and Rock Deformation, Laboratory Studies—The Paterson Volume* (edited by Hobbs, B. E. & Heard, H. C.). *Am. Geophys. Un. Geophys. Monogr.* **36**, 51–72.

Passchier, C. W. & Simpson, C. 1986. Porphyroclast systems as kinematic indicators. *J. Struct. Geol.* **8**, 831–843.

Patterson, S. R., Vernon, R. H. & Tobish, O. T. 1989. A review of the criteria for the identification of magmatic and tectonic foliations. *J. Struct. Geol.* **11**, 349–363.

Pfiffner, O. A. & Ramsay, J. G. 1982. Constraints on geological strain rates: Arguments from finite strain states of naturally deformed rocks. *J. geophys. Res.* **87-B1**, 311–321.

Poirier, J. P. 1985. *Creep of Crystals—High Temperature Deformation Processes in Metals, Ceramics and Minerals*. Cambridge University Press, New York.

Puls, D. D. 1986. Geometric and kinematic analysis of a Proterozoic foreland thrust belt, northern Mazatzal Mountains, central Arizona. Unpublished M.S. thesis, Northern Arizona University.

Ralser, S., Hobbs, B. E. & Ord, A. 1991. Experimental deformation of a quartz mylonite. *J. Struct. Geol.* **13**, 837–850.

Ramsay, J. G. & Huber, M. I. 1983. *The Techniques of Modern Structural Geology, Volume* 1: *Strain Analysis*. Academic Press, New York.

Ratte', J. C., Marvin, C. W., Naeser, C. W. & Bikerman, M. 1984. Calderas and ash flow tuffs of the Mogollon Mountains, southwestern New Mexico. *J. geophys. Res.* **89**, 8713–8732.

Rhodes, R. C. 1976. Volcanic geology of the Mogollon Range and adjacent areas, Catron and Grant counties, New Mexico. In: *Cenozoic Volcanism* (edited by Elston, W. E. & Northrop, S. A.). *Spec. Publ. New Mexico geol. Soc.* **5**, 42–50.

Rhodes, R. C. & Smith, E. I. 1972. Distribution and directional fabric of ash flow tuff sheets in the northwestern Mogollon Plateau, New Mexico. *Bull. geol. Soc. Am.* **83**, 1863–1868.

Robertson, J. M. & Condie, K. C. 1989. Geology and geochemistry of early Proterozoic volcanic and subvolcanic rocks of the Pecos greenstone belt, Sangre de Cristo Mountains, New Mexico. In: *Proterozoic Geology of the Southern Rocky Mountains* (edited by Grambling, J. A. & Tewksbury, B. J.). *Spec. Pap. geol. Soc. Am.* **235**, 119–146.

Robertson, J. M., Grambling, J. A., Mawer, C. K., Williams, M. L., Bauer, P. W. & Silver, L. T. In press. Precambrian of New Mexico.

In: *Precambrian Rocks of North America* (edited by Van Schmus, R. & Bickford, M. P.). Geological Society of America, Decade of North American Geology.
Schmid, S. M. 1976. Rheological evidence for changes in the deformation mechanism of Solenhofen limestone towards low stress. *Tectonophysics* **31**, T21–T28.
Schmid, S. M. & Casey, M. 1986. Complete fabric analysis of some commonly observed *c*-axis patterns. In: *Mineral and Rock Deformation, Laboratory Studies—The Paterson Volume* (edited by Hobbs, B. E. & Heard, H. C.). *Am. Geophys. Un. Geophys. Monogr.* **36**, 263–286.
Schmincke, H-U. & Swanson, D. A. 1967. Laminar viscous flowage structures in ash-flow tuffs from Gran Canaria, Canary Islands. *J. Geol.* **75**, 641–664.
Seaman, S. J. & Williams, M. L. 1992. Center-to-center analyses and flow fabric characterization in ash-flow tuffs. *Bull. Volcanol.* **54**, 319–328.
Smith, R. L. 1979. Ash-flow magmatism. In: *Ash Flow Tuffs* (edited by Chapin, C. E. & Elston, W. E.). *Spec. Pap. geol. Soc. Am.* **180**, 5–27.
Spry, A. 1969. *Metamorphic textures*. Pergammon Press, New York.
Stanton, 1976. Petrochemical studies of the ore environment at Broken Hill, South Wales: 2-regional metamorphism of banded iron formations and their immediate associates. *Trans. Instn Min. Metall.* **85**, B118–B131.
Swanson, S. E. & Fenn, P. 1986. Quartz crystallization in igneous rocks. *Am. Mineral.* **71**, 337–342.
Thompson, A. G., Grambling, J. A. & Dallmeyer, R. D. 1991. Proterozoic tectonic history of the Manzano Mountains, central New Mexico. In: *Field Guide to Geologic Excursions in New Mexico and Adjacent Areas of Texas and Colorado* (edited by Julian, B. & Zidek, J.). *Bull. New Mexico Bur. Mines & Mineral resourc.* **137**, 71–77.
Thorpe, D. G. 1980. Mineralogy and petrology of precambrian metavolcanic rock, Squaw Peak, Arizona. Unpublished M.S. thesis, Arizona State University.
Thorpe, D. G. & Burt, D. M. 1978. Precambrian metavolcanic rocks of the Squaw Peak area, Maricopa County, Arizona. *Spec. Rep. Arizona Bur. Geol. & Miner. Technol.* **2**, 101–106.
Vernon, R. H. 1976. *Metamorphic Processes—Reactions and Microstructure Development*. George Allen and Unwin, Boston.
Vernon, R. H. 1986a. Evaluation of the "quartz eye" hypothesis. *Econ. Geol.* **81**, 1520–1527.
Vernon, R. H. 1986b. K-feldspar megacrysts in granites—phenocrysts, not porphyroblasts. *Earth Sci. Rev.* **23**, 1–63.
Vernon, R. H. & Flood, R. H. 1977. "Quartz-eye"-bearing porphyroidal rocks and volcanogenic massive sulfide deposits—a discussion. *Econ. Geol.* **72**, 698–701.
Walker, G. P. L. 1983. Ignimbrite types and ignimbrite problems. *J. Volcanol. & Geotherm. Res.* **17**, 65–88.
White, S. 1975. Tectonic deformation and recrystallization of plagioclase. *Contr. Miner. Petrol.* **50**, 287–304.
White, S. 1976. The effects of strain on the microstructure, fabrics, and deformation mechanisms in quartzite. *Phil. Trans. R. Soc. Lond.* **A283**, 69–86.
Williams, M. L. 1987. Stratigraphic, structural, and metamorphic relationships in Proterozoic rocks from northern New Mexico. Unpublished Ph.D. thesis, University of New Mexico.
Williams, M. L. 1990. Proterozoic geology of northern new Mexico: recent advances and ongoing questions. In: *Geology of the Southern Rocky Mountains* (edited by Bauer, P. W. & Mawer, C. K.). *New Mexico geol. Soc. Guidebook* **41**, 151–159.
Williams, M. L. 1991a. Heterogeneous deformation in a ductile fold-thrust belt: the Proterozoic tectonic history of the Tusas Mountains, New Mexico. *Bull. geol. Soc. Am.* **103**, 171–188.
Williams, M. L. 1991b. Overview of Early Proterozoic Metamorphism in Arizona. In: *Proterozoic Geology and Ore Deposits of Arizona* (edited by Karlstrom, K. E.). *Arizona geol. Soc. Digest* **19**, 11–26.
Williams, M. L. & Burr, J. L. 1990. Preservation of quartz phenocrysts and kinematic indicators in metamorphosed and deformed Proterozoic rhyolites, southwestern North America. *Geol. Soc. Am. Abs. w. Prog.* **22**, 139.
Wolff, J. A. & Wright, J. V. 1981. Rheomorphism of welded tuffs. *J. Volcanol. & Geotherm. Res.* **10**, 13–34.